Clearance of persistent hepatitis C virus infection in humanized mice using a claudin-1-targeting monoclonal antibody

Mailly, L. , Xiao, F. , Lupberger, J. , Wilson, G.K. , Aubert, P. , Duong, F.H.T. , Calabrese, D. , Leboeuf, C. , Fofana, I. , Thumann, C. , Bandiera, S. , Lütgehetmann, M. , Volz, T. , Davis, C. , Harris, H.J. , Mee, C. , Girardi, E. , Chane-Woon-Ming, B. , Ericsson, M. , Fletcher, N. , Bartenschlager, R. , Pessaux, P. , Vercauteren, K. , Meuleman, P. , Villa, P. , Kaderali, L. , Pfeffer, S. , Heim, M.H. , Neunlist, M. , Zeisel, M.B. , Dandri, M. , McKeating, J.A. , Robinet, E. and Baumert, T.F.

Original citation & hyperlink:
Mailly, L. , Xiao, F. , Lupberger, J. , Wilson, G.K. , Aubert, P. , Duong, F.H.T…. Baumert, T.F. (2015) Clearance of persistent hepatitis C virus infection in humanized mice using a claudin-1-targeting monoclonal antibody. Nature Biotechnology, volume 33 : 549-554.
http://dx.doi.org/10.1038/nbt.3179

Supplementary materials: http://www.nature.com/nbt/journal/v33/n5/extref/nbt.3179-S1.pdf

Additional note: The different title on page 2 of this document is due to a title change being made to the paper between peer-review and publication.

Clearance of persistent hepatitis C virus infection using a monoclonal antibody specific for tight junction protein claudin-1

Laurent Mailly[1, 2], Fei Xiao[1, 2, *], Joachim Lupberger[1, 2, *], Garrick K. Wilson[3], Philippe Aubert[4, 5, 6], François H. T. Duong[7], Diego Calabrese[7], Céline Leboeuf[1, 2], Isabel Fofana[1, 2], Christine Thumann[1, 2], Simonetta Bandiera[1, 2], Marc Lütgehetmann[8], Tassilo Volz[8], Christopher Davis[3], Helen J. Harris[3], Christopher Mee[3], Erika Girardi[2, 9], Béatrice Chane-Woon-Ming[2, 9], Maria Ericsson[10], Nicola Fletcher[5], Ralf Bartenschlager[11, 12], Patrick Pessaux[1, 2, 13], Koen Vercauteren[14], Philip Meuleman[14], Pascal Villa[2, 15], Lars Kaderali[16], Sébastien Pfeffer[2, 9], Markus H. Heim[7], Michel Neunlist[4, 5, 6], Mirjam B. Zeisel[1, 2], Maura Dandri[8], Jane A. McKeating[3], Eric Robinet[1, 2, §] and Thomas F. Baumert[1, 2, 13, §]

[1]Institut National de la Santé et de la Recherche Médicale, U1110, Strasbourg, France; [2]Université de Strasbourg, Strasbourg, France; [3]Hepatitis C Research Group, Institute for Biomedical Research, University of Birmingham, Birmingham, United Kingdom; [4]Institut National de la Santé et de la Recherche Médicale, U913, Nantes, France; [5]Université de Nantes, Nantes, France; [6]Institut des Maladies de l'Appareil Digestif, CHU Nantes, Hôpital Hôtel-Dieu, Nantes, France; [7]Department of Biomedicine, Hepatology Laboratory, University of Basel, Basel, Switzerland; [8]I. Department of Internal Medicine, University Medical Center Hamburg-Eppendorf, Hamburg, Germany; [9]Architecture et Réactivité de l'ARN, Institut de Biologie Moléculaire et Cellulaire du

CNRS – UPR 9002, Strasbourg, France; [10]Electron Microscopy Facility, Harvard Medical School, Boston, USA; [11]Department of Infectious Diseases, Molecular Virology, Heidelberg University, Heidelberg, Germany; [12]German Centre for Infection Research, Heidelberg University, Heidelberg, Germany; [13]Pôle Hépato-Digestif, Institut Hopitalo-Universitaire, Hôpitaux Universitaires de Strasbourg, Strasbourg, France; [14]Center for Vaccinology, Ghent University and Hospital, Ghent, Belgium; [15]Plateforme de Chimie Biologique Intégrative de Strasbourg, UMS 3286 CNRS-UdS & FMTS, Illkirch, France; [16]Institute for Medical Informatics and Biometry, Medical Faculty, Technische Universität Dresden, Dresden, Germany.

*These authors contributed equally to the work.

[§]These authors contributed equally to the work.

Correspondence should be addressed to:

Prof. Thomas F. Baumert, MD, Institut National de la Santé et de la Recherche Médicale U1110, Institut de Recherche sur les Maladies Virales et Hépatiques, Université de Strasbourg, 3 rue Koeberlé, 67000 Strasbourg, France. Email: thomas.baumert@unistra.fr

Prevention and cure of infectious diseases remain a major challenge. Hepatitis C virus (HCV) infection is a leading cause of liver cirrhosis and cancer[1]. Tight junction (TJ) proteins mediate cell entry of HCV[2,3] and other pathogens including dengue virus, coxsackievirus, adenovirus and shigella[4-7]. However, the role of TJ proteins as therapeutic targets is unknown. Using a human liver-chimeric mouse model[8-10] we report that a monoclonal antibody specific for TJ protein claudin-1[11] eliminates chronic HCV infection with undetectable toxicity. This antibody inhibits HCV entry, cell-cell transmission and virus-induced signaling events. Importantly, antibody treatment reduces the frequency of HCV-infected hepatocytes *in vivo*, highlighting the need for *de-novo* infection via host entry factors to maintain chronic infection. In summary, we demonstrate that an antibody targeting a virus receptor can cure chronic viral infection and uncover TJ proteins as targets for antiviral therapy, highlighting this novel host-targeting strategy for a broad range of pathogens.

Word count: introductory paragraph 150 words, main text 2,817 words, methods 1,614 words

The tight junction (TJ) proteins claudin-1 (CLDN1) and occludin have been shown to mediate hepatitis C virus (HCV) entry into host cells[2,3]. TJs have also been implicated in the entry of several other pathogens including dengue virus[7], adenovirus[4], coxsackievirus[5] and shigella[6]. Although these reports demonstrate a role for TJ proteins in the life cycle of a broad range of pathogens, their role in viral pathogenesis and as targets for antiviral therapy are unknown. To address this question we used a recently developed CLDN1-specific monoclonal antibody (mAb)[11] and the human chimeric uPA-SCID mouse model[8] to evaluate the therapeutic potential of this mAb to control acute and chronic HCV infection. Owing to discontinuation of research in chimpanzees for ethical reasons, this mouse model is the only available model that supports robust long-term chronic HCV infection. Although these mice lack a functional immune system that precludes the study of immune-mediated events, this mouse model has contributed significantly to our understanding of viral pathogenesis, validation of antiviral strategies and the assessment of efficacy and safety profiles of antivirals[9,10,12-17].

First, we analyzed CLDN1 expression in the chimeric liver using a commercially available mAb that recognizes human and mouse CLDN1 (Supplementary Fig.1). Confocal imaging demonstrated that the majority of CLDN1 on human hepatocytes co-localized with apical marker CD10 demonstrating the formation of bile canalicular structures (Fig.1a). A minor pool of protein was detected at the basolateral membrane as identified with cytokeratin-8 staining (Fig.1a, data not shown and [18]). Comparative staining of normal human liver tissue demonstrated comparable subcellular localization

(Fig.1a). Transmission electron microscopic (TEM) analysis confirmed that hepatocytes in the chimeric mouse liver form TJs that were structurally indistinguishable from those in human liver tissue (Supplementary Fig.2a-b). The similar localization of hepatocellular CLDN1 and hepatocyte architecture suggests that the uPA-chimeric mouse is a relevant model to evaluate CLDN1 as a therapeutic target. Next, we characterized the subcellular localization of CLDN1 recognized by the CLDN1-specific mAb (OM-7D3-B3) used in our mouse challenge studies. TEM and immunogold labeling of *in vivo* administered CLDN1-specific mAb showed reactivity with basolateral and sinusoidal hepatocyte membranes *in vivo* (Fig.1b), whereas we failed to detect staining of tight junctions (Fig.1b). Basolateral membrane staining was confirmed using live cell imaging of polarized HepG2 cells – a physiologically relevant cell line frequently used to study HCV entry (Fig.1c)[19,20]. Collectively, these data suggest that the CLDN1-specific mAb predominantly binds to non-junctional pools of CLDN1 on the hepatocyte basolateral membrane *in vivo*.

To investigate the antiviral effect of our CLDN1-specific mAb, chimeric uPA-SCID mice received CLDN1-specific (n=5) or control isotype matched irrelevant mAb (n=4) one day prior to inoculation, and 1 and 5 days post infection with a primary HCV genotype 1b serum. The CLDN1-specific mAb provided a complete and sustained protection from infection as evidenced by undetectable HCV RNA in the sera for up to 6 weeks post-infection (Fig.2a, Supplementary Table 1). In contrast, all control mAb-treated mice became infected (Fig.2a). Similar results were observed following infection

with a HCV of the difficult-to-treat genotype 4 (isolate ED43[21], Fig.2b, Supplementary Table 1) demonstrating a significant level of anti-viral activity ($p< 0.0002$, pooled data from experiments of both genotypes, Mann-Whitney test). Pharmacokinetic studies showed that CLDN1-specific mAb levels declined rapidly and were undetectable 2 weeks after administration (Fig.2f-g). Collectively, these data show that short-term administration of a CLDN1-specific mAb prevents *de novo* HCV infection and highlights a new opportunity to prevent HCV re-infection during liver transplantation.

To investigate the effect of the CLDN1-specific mAb on chronic HCV infection we utilized mice persistently infected with the cell culture-derived HCV (HCVcc) strain Jc1 (genotype 2a/2a chimera)[22], a prototype strain based on JFH1[23] that is used extensively to study virus-host interactions and to evaluate antivirals *in vitro* and *in vivo*[22-26]. Persistently infected mice (24 to 50 days post-infection) were given 4 weekly doses of CLDN1-specific (n=5) or control mAb (n=4). All CLDN1-specific mAb-treated mice showed undetectable HCV RNA levels after 2 to 4 injections (Fig.2c, Supplementary Table 1) and, except for one case, animals remained virus free until the end of the study period. The exception being one mouse that showed a relapse (Fig.2c, Supplementary Table 1), associating with low levels of antibody during the early treatment phase (Fig.2h). However, low levels of mAbs did not always correlate with relapse (Fig.2i-j). Sequencing and functional analysis of viral envelope glycoproteins from antibody-treated mice in HCVpp and HCVcc (Supplementary Fig.3a-e) suggested that the relapse was unlikely to be explained by the presence of resistant variants that escaped

the CLDN1-specific mAb (Supplementary Fig.3c-d) or to CLDN1-independent cell entry (Supplementary Fig.3e). Of note, human hepatocytes engrafted into upA-SCID mice expressed lower levels of CLDN6 than Huh7.5.1 cells used for escape studies (Supplementary Fig.4a-d). These data suggest that the absent escape observed in the HCV-Huh7.5.1 cell culture model expressing high levels of CLDN6 is relevant for HCV infection *in vivo*. The mAb concentration peaked during the treatment period and declined rapidly following discontinuation of mAb injection (Fig.2h). Similar results were observed in 4 additional Jc1-infected CLDN1-specific mAb-treated mice with follow-up of 3 weeks (data not shown). CLDN1 mAb induced viral clearance from mice chronically infected with HCVcc VL-JFH1 (genotype 1b/2a chimera) (n=5), a well characterized strain[27] encoding the structural proteins from a highly infectious HCV neutralization escape variant isolated from a patient undergoing liver transplantation[12] (Fig.2d, Supplementary Table 1). One mouse showing a partial viral response (Fig.2d, Supplementary Table 1) was characterized by undetectable mAb concentration after the second injection (Fig.2i). The therapeutic effect was robust (HCV RNA decline > 2 logs), sustained (until the end of the study period corresponding to 11 weeks) and significant ($p< 0.0007$, pooled data for experiments of both genotypes, Mann-Whitney test). Furthermore, a similar effect was observed in mice chronically infected with a genotype 2a serum confirming the antiviral activity using an inoculum with high viral diversity (Fig.2e, Supplementary Table 1). Mice infected with primary isolates of genotype 4 (n=4) also showed a marked and time-dependent decrease in HCV RNA levels (Supplementary Fig.5a) with no viral rebound and stable function of the engrafted

human hepatocytes as shown by serum albumin levels (Supplementary Fig.5b). In summary, these data show that a CLDN1-specific mAb can clear chronic HCV infection *in vivo* and exhibits antiviral activity against different viral genotypes. These findings uncover a TJ protein as a therapeutic target in a clinically relevant animal model and highlight a previously unknown property of an inhibitor targeting a cell entry factor.

To assess antibody safety, we analyzed the histopathology of chimeric livers from uPA-SCID mice. Human hepatocyte-specific staining demonstrated similar repopulation and structure of human hepatocytes in HCV Jc1-infected mice treated with control or CLDN1-specific mAb (Supplementary Fig.6a). TEM analysis of chimeric infected livers of treated mice showed no detectable alteration in hepatocyte morphology or TJ ultra-structure (data not shown). Human albumin, transaminases (ALT, AST) and total bilirubin levels remained stable following antibody administration and were similar in control and CLDN1 mAb-treated mice at all time points tested (Supplementary Fig.6b-e). To assess the functional integrity of human hepatocytes in CLDN1 mAb-treated mice we challenged the mice with HCV of a different strain and genotype. Indeed, CLDN1 mAb-treated animals previously protected from HCV infection (Fig.2a) supported viral infection following elimination of the CLDN1-specific mAb (Supplementary Fig.6f). These functional data corroborate the presence of fully viable and functional hepatocytes following anti-CLDN1 treatment and exclude adverse effects on hepatocyte function *in vivo*.

To address potential side effects of the CLDN1-specific mAb in other organs and tissues we assessed antibody binding to human and murine CLDN1 (Supplementary Fig.7a-g). The antibody bound primary mouse hepatocytes and 293T cells expressing murine CLDN1 with an apparent Kd of 83.6 ± 14.1 nM compared to the apparent Kd for human CLDN1 expressed in 293T cells (17.05 ± 1.14 nM) (Supplementary Fig.7g). Moreover, the latter was in a similar range as the Kd of CLDN1-specific mAb binding to human hepatocytes[11]. Next we measured *in vivo* biodistribution in Balb/c and observed enrichment in skin, kidneys, lungs, intestines and liver (Supplementary Fig.9a-b). Toxicity studies in Balb/c mice including clinical (data not shown), biochemical and hematological parameters such as blood counts, liver and kidney function tests as well as histopathological analyses did not reveal toxicity in any of the analyzed organs (Supplementary Fig.8, Supplementary Tables 2, 3). Since TJs play a key role in intestinal paracellular permeability, we investigated the effect of our CLDN1-specific mAb on intestinal barrier function *in vivo*. The CLDN1-specific mAb had no effect on intestinal paracellular permeability (Supplementary Fig.9c) or total intestinal transit time (Supplementary Fig.9d), in contrast to irradiated mice that were used as positive control. Additional *ex vivo* studies showed that the CLDN1-specific antibody had no detectable effects on paracellular permeability (Supplementary Fig.9e) or tissue conductance in the small intestine or colon (Supplementary Fig.9f). Intestinal epithelial barrier function upon CLDN1-specific mAb administration was further confirmed *in vitro* by demonstrating that the mAb had no effect on the gut intestinal Caco-2 trans-epithelial electrical resistance (Supplementary Fig.9g) that are known to express abundant levels of CLDN1

(Supplementary Fig.9h). We confirmed that the antibody had no effect on TJ function in the hepatic HepG2 model system[28]. While CLDN1 knock-down significantly reduced TJ integrity in a model of polarized HepG2 cells (Supplementary Fig.10a-b), the CLDN1-specific mAb had no impact (Supplementary Fig.10c). Furthermore, flow cytometry experiments measuring CLDN1 cell surface expression suggested that the CLDN1-specific mAb did not promote cellular CLDN1 internalization (Supplementary Fig.10d). Finally, a detailed analysis of cytokine mRNA expression in antibody-treated mice did not reveal evidence for antibody-induced inflammatory changes in the mouse jejunum (data not shown). Collectively, these data exclude major toxicity or side effects induced by the CLDN1-specific mAb in mice. Due to the absent interaction of the rat antibody with the mouse Fc receptor, immune-mediated adverse effects, e.g. ADCC, cannot be assessed in this model. Humanization of the antibody using an IgG4 backbone – a well established strategy to minimize ADCC[29,30] – is underway for its clinical development.

To explore the antiviral mechanism of the CLDN1-specific mAb, we performed both *in vitro* and *in vivo* studies. Using protein association studies and a Förster resonance energy transfer (FRET)-based assay, we found that the CLDN1-specific mAb interfered with CD81-CLDN1 co-receptor complex formation (Supplementary Fig.11a) - a key step required for HCV entry[19]. Co-receptor perturbation most likely occurs at the hepatocyte basolateral membrane as shown by immunofluorescence studies of polarized HepG2 cells or immunogold affinity labeling of hepatocytes (Fig.1b-c). Furthermore, we demonstrate that the CLDN1-specific mAb significantly inhibits cell-

free and cell-cell routes of transmission[31] (Supplementary Fig.11b-e). Of note, inhibition of cell-cell transmission led to a marked decrease of virus spread in the hepatoma cell culture model when the CLDN1-specific mAb was added 48h post-infection (Supplementary Fig.11e). The ability of the antibody to inhibit cell-free and cell-cell infection may explain, at least in part, the antiviral effects of the CLDN1-specific mAb to cure persistent HCV infection *in vivo.* Since this mAb neither impaired HCV replication nor assembly/release (Supplementary Fig.11f-g), we conclude that the mAb acts predominantly by interfering with HCV entry.

Since CLDNs have been shown to play a role in modulating miRNA expression and signaling pathways[32,33], we investigated whether the antibody modulated the miRNA and kinome profile of persistent HCV-infected Huh7.5.1 cells. Consistent with previous observations[34] our deep sequencing studies confirmed that HCV infection modulates miRNA profiles in Huh7.5.1 cells. However, the CLDN1-specific mAb had no detectable effect on miRNA expression (Supplementary Fig.12).

HCV binding to hepatocellular CD81 and associated receptors activates EGFR and mitogen-activated protein kinase (MAPK) pathway signaling[35,36]. HCV (Jc1) infection increased Erk1/2 phosphorylation and this was reversed by the CLDN1-specific mAb (Fig.3a-b). The significance of HCV-induced MAPK signaling was supported by analyzing liver biopsies from HCV infected patients (Fig.3c-d, Supplementary Table 4, $p< 0.05$, Mann-Whitney test). Importantly, we observed an antiviral effect of small molecule inhibitors targeting MAPK signaling (Fig.3e) at non

toxic concentrations[10,37] (Supplementary Table 5). To confirm the effect of the CLDN1-specific mAb on HCV-induced signaling in liver tissue from HCV-infected patients (Supplementary Table 4), freshly isolated liver biopsies were treated *ex vivo* with CLDN1-specific or control mAb and we observed a reduction of Erk1/2 phosphorylation compared to control-treated biopsies (Fig.3f). These studies show that HCV infection activates MAPK signaling and CLDN1-specific mAb partially reverses this virus-dependant signaling event without impairing Erk activation by the physiological EGFR ligand EGF (Fig.3g-h). Collectively these data suggest a model in which the anti-CLDN1 mAb prevents the HCV-induced cross-activation of EGFR and Erk by interfering with CD81-CLDN1 association (Fig.3i). Since MAPK signaling pathway has been shown to play an essential role in the HCV life cycle, including viral entry[37,38], it is likely that this interference contributes to the ability of the mAb to clear an established infection.

Finally, we performed mechanistic studies in human chimeric mice to study the consequences of the observed mechanistic findings for viral clearance *in vivo*. Using FISH with HCV- and human GAPDH-RNA specific probes (Fig.4a) we demonstrate that CLDN1-mAb results in a dose- and time-dependent decrease in the number of HCV-infected cells leading to their final elimination (Fig.4b). Furthermore, the decline of HCV-infected hepatocytes paralleled the decline in peripheral HCV RNA levels, showing a monophasic decline (Fig.4b, Supplementary Fig.13). Of note, the baseline frequency of HCV-infected hepatocytes (Fig. 4b) in the chimeric mouse liver were comparable to those reported in the chronically infected human liver[39].

Assuming an inhibition of entry of > 99% at mAb serum concentrations exceeding 100 ug/mL (as shown in Supplementary Fig.11) and a negligible effect on viral genome replication and/or assembly (Supplementary Fig.11f-g), mathematic modeling predicts a time-dependent elimination of virus-infected hepatocytes with concomitant absent *de-novo*-infection. Applying this model, we estimated the half-life of infected cells to be ~ 1.3 days for genotype 2a and 5.4 days for genotype 4 which is in the range of hepatocytes half-lives reported in patients[40]. Indeed, HCV has been reported to promote cellular apoptosis *in vitro* and *in vivo* (Supplementary Fig.14 and [41,42]). During serum HCV RNA decline, virus infected hepatocytes are constantly replaced by non-infected hepatocytes, as shown by very stable human albumin levels (Supplementary Figs.5b, 6b), resulting in viral control and clearance. This model is supported by both FISH analyses of liver tissue sections (Fig.4) and *in vitro* studies where CLDN1-specific mAb eliminates HCV-infected cells (Supplementary Fig.14c-d). The different half-lives of HCV-infected cells and the magnitude of virus-induced cell death may explain the varying magnitude of the decline in viral load for diverse HCV strains (Supplementary Figs.5a, 13)[40].

In contrast to previous studies reporting on CD81- and SR-BI-specific antibodies preventing virus infection of human chimeric mice[9,14], we demonstrate for the first time that a host-targeting entry inhibitor clears chronic viral infection (Fig.2c-e). Our results show that viral entry and spread are required for persistent infection *in vivo* and that TJ protein CLDN1 is a valid target to both prevent and treat chronic HCV infection. The

interaction of the mAb with non-junctional pools of CLDN1 (Fig.1b-c) that complex with the viral co-receptor CD81 (Supplementary Fig.11a), may explain the non-detectable toxicity (Supplementary Figs.6a-f, 8, 9c-g, Supplementary Tables 2, 3). This is in line with our results showing a specific role for the CLDN1-specific mAb to perturb MAPK signaling events in infected cells and liver tissue but to have no effect on naïve target cells (Fig.3a-b, f).

In summary, therapeutic administration of a CLDN1-specific mAb demonstrates broad and marked activity against several genotypes (Fig.2, Supplementary Fig.5, 11b) without detectable toxicity as determined by structural, biochemical and functional assays (Supplementary Figs.6, 8, 9, Supplementary Tables 2, 3). The absence of detectable viral resistance (Supplementary Fig.3) suggests that CLDN1 is an antiviral target with a high genetic barrier for resistance. Although a recent report described strain-dependent use of CLDN1 and 6 in hepatoma cell lines *in vitro*[43], our *in vivo* data suggest that the antiviral effect of the CLDN1-specific mAb is independent of viral strain, genotype and hepatocyte donors (Fig.2, Supplementary Figs.5a, 11b). Collectively, these data suggest that CLDN1 is essential for HCV infection *in vivo* and that low expression levels of CLDN6 and CLDN9 in human hepatocytes (Supplementary Fig.4 and [43,44]) preclude a relevant entry function of these molecules *in vivo*.

In contrast to direct-acting antivirals in clinical use or development, the CLDN1-specific mAb eliminates viral infection in monotherapy in the current state-of-the-art

animal model (Fig.2, Supplementary Fig.5a) and does not result in detectable resistance (Supplementary Fig.3). We predict that these features are due to its unique mechanism of action targeting a host cell factor (Supplementary Fig.11a) that is essential for viral persistence *in vivo* as well as modulating host cell signaling of virus-infected cells (Fig.3) likely contributing to clearance. Collectively, these data suggest that antibodies or small molecules targeting CLDN1 are promising candidates to prevent liver graft infection and to eliminate chronic HCV infection. Finally, our proof-of-concept study uncovering CLDN1 as target for cure of HCV infection allows the design of novel antimicrobial strategies for a broad range of viruses and pathogens that utilize TJ proteins as host factors including dengue virus, coxackievirus, adenovirus and shigella [4-7].

REFERENCES

1. Thomas, D.L. Global control of hepatitis C: where challenge meets opportunity. Nat Med 19, 850-858 (2013).
2. Evans, M.J., et al. Claudin-1 is a hepatitis C virus co-receptor required for a late step in entry. Nature 446, 801-805 (2007).
3. Ploss, A., et al. Human occludin is a hepatitis C virus entry factor required for infection of mouse cells. Nature 457, 882-886 (2009).
4. Cohen, C.J., et al. The coxsackievirus and adenovirus receptor is a transmembrane component of the tight junction. Proc Natl Acad Sci U S A 98, 15191-15196 (2001).
5. Coyne, C.B. & Bergelson, J.M. Virus-induced Abl and Fyn kinase signals permit coxsackievirus entry through epithelial tight junctions. Cell 124, 119-131 (2006).
6. Fukumatsu, M., et al. Shigella targets epithelial tricellular junctions and uses a noncanonical clathrin-dependent endocytic pathway to spread between cells. Cell Host Microbe 11, 325-336 (2012).
7. Che, P., Tang, H. & Li, Q. The interaction between claudin-1 and dengue viral prM/M protein for its entry. Virology 446, 303-313 (2013).
8. Mercer, D.F., et al. Hepatitis C virus replication in mice with chimeric human livers. Nat Med 7, 927-933 (2001).
9. Law, M., et al. Broadly neutralizing antibodies protect against hepatitis C virus quasispecies challenge. Nat Med 14, 25-27 (2008).

10. Lupberger, J., et al. EGFR and EphA2 are host factors for hepatitis C virus entry and possible targets for antiviral therapy. Nat Med 17, 589-595 (2011).

11. Fofana, I., et al. Monoclonal anti-claudin 1 antibodies prevent hepatitis C virus infection of primary human hepatocytes. Gastroenterology 139, 953-964.e954 (2010).

12. Fafi-Kremer, S., et al. Viral entry and escape from antibody-mediated neutralization influence hepatitis C virus reinfection in liver transplantation. J Exp Med 207, 2019-2031 (2010).

13. Meuleman, P., et al. Anti-CD81 antibodies can prevent a hepatitis C virus infectionin vivo. Hepatology 48, 1761-1768 (2008).

14. Meuleman, P., et al. A human monoclonal antibody targeting scavenger receptor class B type I precludes hepatitis C virus infection and viral spread in vitro and in vivo. Hepatology 55, 364-372 (2012).

15. Petersen, J., et al. Prevention of hepatitis B virus infection in vivo by entry inhibitors derived from the large envelope protein. Nat Biotechnol 26, 335-341 (2008).

16. Hiraga, N., et al. Infection of human hepatocyte chimeric mouse with genetically engineered hepatitis C virus and its susceptibility to interferon. FEBS Lett 581, 1983-1987 (2007).

17. Shi, N., et al. Combination therapies with NS5A, NS3 and NS5B inhibitors on different genotypes of hepatitis C virus in human hepatocyte chimeric mice. Gut (2013).

18. Harris, H.J., Wilson, G.K., Hubscher, S.G. & McKeating, J.A. Heterogeneous claudin-1 expression in human liver. Hepatology 57, 854-855 (2013).

19. Harris, H.J., et al. Claudin association with CD81 defines hepatitis C virus entry. J Biol Chem 285, 21092-21102 (2010).

20. Fletcher, N.F., et al. Activated macrophages promote hepatitis C virus entry in a tumor necrosis factor-dependent manner. Hepatology 59, 1320-1330 (2014).

21. Bukh, J., et al. Challenge pools of hepatitis C virus genotypes 1-6 prototype strains: replication fitness and pathogenicity in chimpanzees and human liver-chimeric mouse models. J Infect Dis 201, 1381-1389 (2010).

22. Pietschmann, T., et al. Construction and characterization of infectious intragenotypic and intergenotypic hepatitis C virus chimeras. Proc Natl Acad Sci U S A 103, 7408-7413 (2006).

23. Wakita, T., et al. Production of infectious hepatitis C virus in tissue culture from a cloned viral genome. Nat Med 11, 791-796 (2005).

24. Lindenbach, B.D., et al. Complete replication of hepatitis C virus in cell culture. Science 309, 623-626 (2005).

25. Lindenbach, B.D., et al. Cell culture-grown hepatitis C virus is infectious in vivo and can be recultured in vitro. Proc Natl Acad Sci U S A 103, 3805-3809 (2006).

26. Zhong, J., et al. Robust hepatitis C virus infection in vitro. Proc Natl Acad Sci U S A 102, 9294-9299 (2005).

27. Fofana, I., et al. Mutations that alter use of hepatitis C virus cell entry factors mediate escape from neutralizing antibodies. Gastroenterology (2012).

28. Krieger, S.E., et al. Inhibition of hepatitis C virus infection by anti-claudin-1 antibodies is mediated by neutralization of E2-CD81-claudin-1 associations. Hepatology 51, 1144-1157 (2010).

29. Dübel, S. & Reichert, J.M. (eds.). Handbook of Therapeutic Antibodies, 2544 (Wiley-Blackwell, 2014).

30. Yang, X. & Ambrogelly, A. Enlarging the repertoire of therapeutic monoclonal antibodies platforms: domesticating half molecule exchange to produce stable IgG4 and IgG1 bispecific antibodies. Curr Opin Biotechnol 30C, 225-229 (2014).

31. Brimacombe, C.L., et al. Neutralizing antibody-resistant hepatitis C virus cell-to-cell transmission. J Virol 85, 596-605 (2011).

32. Gong, Y., et al. Claudin-14 regulates renal Ca(+)(+) transport in response to CaSR signalling via a novel microRNA pathway. EMBO J 31, 1999-2012 (2012).

33. Suh, Y., et al. Claudin-1 induces epithelial-mesenchymal transition through activation of the c-Abl-ERK signaling pathway in human liver cells. Oncogene (2012).

34. Kumar, A. MicroRNA in HCV infection and liver cancer. Biochim Biophys Acta 1809, 694-699 (2011).

35. Brazzoli, M., et al. CD81 is a central regulator of cellular events required for hepatitis C virus infection of human hepatocytes. J Virol 82, 8316-8329 (2008).

36. Diao, J., et al. Hepatitis C virus induces epidermal growth factor receptor activation via CD81 binding for viral internalization and entry. J Virol 86, 10935-10949 (2012).

37. Zona, L., et al. HRas signal transduction promotes hepatitis C virus cell entry by triggering assembly of the host tetraspanin receptor complex. Cell Host Microbe 13, 302-313 (2013).

38. Menzel, N., et al. MAP-kinase regulated cytosolic phospholipase A2 activity is essential for production of infectious hepatitis C virus particles. PLoS Pathog 8, e1002829 (2012).

39. Wieland, S., et al. Simultaneous detection of hepatitis C virus and interferon stimulated gene expression in infected human liver. Hepatology 59, 2121-2130 (2014).

40. Neumann, A.U., et al. Hepatitis C viral dynamics in vivo and the antiviral efficacy of interferon-alpha therapy. Science 282, 103-107 (1998).

41. Lan, L., et al. Hepatitis C virus infection sensitizes human hepatocytes to TRAIL-induced apoptosis in a caspase 9-dependent manner. J Immunol 181, 4926-4935 (2008).

42. Lim, E.J., et al. Hepatitis C-induced hepatocyte cell death and protection by inhibition of apoptosis. J Gen Virol (2014).

43. Haid, S., et al. Isolate-dependent use of Claudins for cell entry by hepatitis C virus. Hepatology (2013).

44. Fofana, I., et al. Functional analysis of claudin-6 and claudin-9 as entry factors for hepatitis C virus infection of human hepatocytes by using monoclonal antibodies. J Virol 87, 10405-10410 (2013).

Acknowledgements. This work was supported by the European Union (ERC-2008-AdG-233130-HEPCENT, ERC-2010-StG-260767-ncRNAVIR) INTERREG-IV-Rhin Supérieur-FEDER-Hepato-Regio-Net 2009 and 2012), ANRS (ANRS 2009/183, 2009/136, 2011/132, 2012/239, 2013/108), ANR (Laboratoires d'excellence HEPSYS, ANR-10-LAB-28 and netRNA ANR-10-LABX-36), Fondation ARC pour la recherche (NanoISI and TheraHCC IHUARC IHU201301187), Institut Hospitalo-Universitaire (IHU) Strasbourg, the Wilhelm Sander Foundation, Région Alsace, Institut National du Cancer, the Institut National de la Santé et de la Recherche Médicale, Centre National de la Recherche Scientifique, Université de Strasbourg, the Ghent University (GOA 01G01712) and the Research Foundation – Flanders (projects 1500910N and G052112N). We are grateful to Dr. S. Ito (Harvard Medical School) for electron microscopy studies, Dr. F.-L. Cosset (Inserm U1111, ENS Lyon, France) and Dr. J. Ball (University of Nottingham, Nottingham, UK) for retroviral vectors for HCVpp production, Dr. F. Chisari (The Scripps Research Institute, La Jolla, USA) for the gift of Huh7.5.1 cells, Dr. A. Patel (MRC Virology Unit, Glasgow, UK) for E2-specific mAb AP33 and Huh7.5-GFP cells, and Drs. C.M. Rice and M. Evans (Rockefeller University and Mount Sinai School of Medicine, New York, NY) for providing human and mouse CLDN1 expression constructs. We acknowledge S. Durand, L. Heydmann, E. Soulier, Dr. J. Barths, N. Brignon, S. Pernot (Inserm U1110, Strasbourg), Drs. O. Wendling and N. Messadeq (ICS, Illkirch), C. Valencia (PCBIS, Illkirch), S. Kallis (University of Heidelberg, Germany) for technical work, Drs. H. Jacob and M.F. Champy (ICS, Illkirch) for histopathological, hematological and biochemical analyzes, Prof. P. Bachellier

(Strasbourg University Hospitals) for providing liver resections for isolation of primary human hepatocytes, the Plateau Technique de Microbiologie, Laboratoire de Virologie, University Hospital Strasbourg for performing part of the viral load analyses, and the IGBMC microarray and sequencing platform, member of the France Génomique program, for the sequencing of our libraries. Part of the animal experiments were carried out within the small animal exploration facility Cardiex (Nantes), which is supported by the GIS-IBiSA program.

Author contributions. T.F.B. initiated and supervised the study. T.F.B., E.R., J.M.K. M.N., M.B.Z., M.H.H., R.B., S.P., and P.V. designed experiments and analyzed data. L.M., P.A., K.V. and E.R. performed *in vivo* experiments and analyzed data. L.M., F.X., J.L., S.B., G.K.W., P.A., F.H.T.D., D.C., C.L., M.E., I.F., C.D., H.J.H., C.T., E.G., B.C.W.M., N.F., M.B.Z. and L.K. performed *ex vivo* and *in vitro* experiments and analyzed data. R.B., P.P. and P.M. provided key reagents. M.D., M.L. and T.V. produced chimeric uPA-SCID mice. L.M., J.L., S.B., M.B.Z., J.M.K., E.R. and T.F.B. wrote the manuscript.

Competing Financial Interests. The authors declare no competing financial interests. Inserm, the University of Strasbourg and Genovac/Aldevron have filed a patent application on monoclonal anti-claudin 1 antibodies for the inhibition of hepatitis C virus infection.

FIGURE LEGENDS

Figure 1. Human CLDN1 expression and tight junction ultrastructure in the livers of human chimeric mice. (**a**) Human CLDN1 expression in non-infected chimeric livers of uPA-SCID mice (left panel) as well as non-infected human livers (right panel) was assessed by confocal microscopy as described in Methods. Representative 3D composite images show human CLDN1 (green) co-stained with apical membrane marker human CD10 (red). Scale bars – 20 µm. (**b**) Binding of CLDN1-specific mAb to hepatocyte ultrastructures was assessed by transmission electron microscopy analyses and immunogold labeling of tissue sections of chimeric human mouse livers from mAb-treated mice. Images show TJ area (left panels) or basolateral membranes of hepatocytes (right panels). Red arrows indicate TJ, empty triangles indicate immunogold staining. Scale bars – 500nm. (**c**) Confocal microscopy of polarized HepG2-CD81 HCV permissive cells stained with CLDN1-specific antibody. HepG2 DsRED-CD81 cells were stained live with CD81- (upper panels) or CLDN1-specific (lower panels) antibodies and visualized by confocal microscopy. CLDN-1 specific staining is predominantly limited to the basolateral membrane of polarized cells. Scale bar – 20µm.

Figure 2. Prevention and clearance of chronic HCV infection using a CLDN1-specific mAb *in vivo*. (**a, b**) Prevention studies. Chimeric uPA-SCID mice received 500 µg CLDN1-specific (n=5) or control mAb (n=4) on days -1, 1 and 5 (arrows) of inoculation (star) with genotype 1b (**a**) or genotype 4 (**b**) HCV-containing serum. One

infected mouse injected with control mAb died on day 26 (**a**, cross). (**c-e**) Treatment studies. Chimeric uPA-SCID mice were chronically infected with HCVcc Jc1[22] (genotype 2a/2a) (**c**), HCVcc VL-JFH1[27] (genotype 1b/2a) (**d**) or serum of genotype 2a (**e**). Twenty-four to 50 days following inoculation, the animals received 500 µg control (**c, d, e**; n=4, 3 and 4 respectively) or CLDN1-specific mAb (**c, d, e**; n=5, 5 and 6 respectively) each week (arrows) for 4 weeks. (**f-j**) Serum concentration of CLDN1-specific mAb from (**a-e respectively**) was determined by ELISA. Serum viral load (**a-e**) was quantified by the clinically licensed Abbott RealTime™ HCV assay. The horizontal dashed line indicates the limit of quantification (LOQ). (**c, d, h, i**) The viral load and antibody concentration of the mice exhibiting a relapse is indicated by a dotted line. Values of individual animals are shown.

Figure 3. CLDN1-specific mAb impairs HCV-induced host cell signaling. (**a**) Detection of kinase phosphorylation in chronically HCV Jc1-infected Huh7.5.1 cells treated with control or CLDN1-specific mAbs (100 µg/mL; 24h) using human phospho-kinase arrays. (**b**) p-Erk1/2 highlighted by black squares in (**a**) was quantified using Image J software (NIH). Results are shown as mean ± s.e.m. of integrated dot blot densities from 2 independent experiments performed in duplicate. (**c**) Erk1/2 phosphorylation is elevated in liver tissue of patients with chronic HCV infection. Expression of p-Erk, total Erk and actin was revealed by Western blotting. (**d**) Quantification of signal intensities of p-Erk1/2 in (**c**) normalized to total Erk expression. Results are shown as the interquartiles (box) with the min and max values (whiskers).

The line within the box indicates the median value. (**e**) Inhibition of the MAPK pathway inhibits persistent HCV infection in Huh7.5.1 cells. Luc-Jc1-infected Huh7.5.1 cells were treated 3 days after inoculation with erlotinib or UO126 (each at 10 µM) for 3 days. HCV replication was assessed by luciferase assay. Results are presented as mean ± s.e.m of 6 independent experiments performed in triplicate. (**f**) CLDN1-specific mAb reduces Erk1/2 phosphorylation in liver tissue from patients with chronic HCV infection. Fresh liver biopsies were divided in two equal pieces and maintained in DMEM medium supplemented with 10% foetal calf serum and 100 µg/mL control or CLDN1-specific mAb for 4h, respectively. Expression of p-Erk, total Erk and actin was determined by Western blotting. Information on liver biopsies is provided in Supplementary Table 4. (**g**) CLDN1-specific mAb does not inhibit EGF-induced Erk1/2 phosphorylation. Huh7.5.1 cells were serum starved for 4h prior 1h incubation with 100 µg/mL control or CLDN1-specific mAb and 15 min incubation with increasing concentrations of EGF. P-EGFR, p-Erk1/2 and total Erk were quantified by Western blotting. (**h**) Quantification of EGF-induced ERK phosphorylation in the presence of CLDN1-specific or control mAb. P-Erk and total Erk Western blot signals described in (**g**) were quantified using a Typhoon Trio laser scanner and ImageQuant Software (GE Healthcare). Values are expressed as relative ratio of p-Erk to total Erk densities (two independent experiments ± s.e.m.). (**i**) Model of HCV-induced signal transduction during cell entry (left panel) and its impairment by CLDN1-specific mAb (right panel). (Left panel) (I) HCV entry is dependent on EGFR signaling which promotes CD81-CLDN1 co-receptor interactions according to Zona et al.[37] and Lupberger et al.[10] (II) At the same time viral binding to the

target cell induces EGFR phosphorylation and signaling via CD81-EGFR interactions as shown by Diao *et al*.[36] and (III) MAPK signaling according to Brazzoli *et al*. by cross-talk[35]. (Right panel) Combining these observations and results shown in panels (**a-h**) and Supplementary Fig.10, our findings are consistent with a model that the CLDN1-specific mAb impairs virus-induced MAPK/Erk signaling by interfering with CD81/CLDN1-MAPK cross-talk without impairing direct EGF-induced Erk phosphorylation. *p<0.05, **p<0.01, ***p<0.0001 (Student's t-test (**b**, **e**), Mann-Whitney test (**d**)).

Figure 4. CLDN1-specific mAb leads to elimination of HCV-infected cells from the livers of human chimeric mice in a dose and time-dependant manner. (**a**) Detection of human hepatocytes and HCV RNA with probes specific for human GAPDH mRNA (green) or HCV Jc1 RNA (red) using FISH. The specificity of the HCV- and GAPDH probes are shown by specific staining of HCV-infected human hepatocytes and absent staining of uninfected human liver (left top panel) and Balb/c mouse liver (right top panel). FISH analyses were then performed in livers of control (left bottom panel) or CLDN1-specific mAb (right bottom panel) treated chimeric uPA-SCID mice. Red arrows indicate HCV positive cells. Scale bar – 50μm. (**b**) Quantification of the percentage of infected cells in the liver of uninfected chimeric mice (black circles) or HCV Jc1-infected mice treated either four times with control mAb (grey triangles), or once (blue diamonds) or four times (blue circles) with CLDN1-specific mAb. Livers were collected 1 week after

the last antibody injection. The quantification was performed after confocal microscopy acquisition.

METHODS

Antibodies. The human CLDN1-specific (OM-7D3-B3, IgG2b, rat[11]), CLDN6-specific (WU-9E1-G2, IgG2b, rat[44]), CLDN9-specific (YD-4E9-A2, IgG2b, rat[44]) mAbs, HCV E2-specific AP33 (mouse)[11], E1-specific IGH433 (human)[11] mAbs and patient-derived HCV-specific IgG[11] have been described. Control mAb (rat IgG2b clone LTF-2, Bio X Cell), Human CLDN1-specific (Life Technologies, rabbit; R&D, rat polyclonal), human CD10-specific (clone 56C6, Vector Laboratories, mouse), human CD81-specific (clone 2s131, mouse), human CK18-specific (clone VP-C414, Vector Laboratories, mouse), Alexa-fluor 488 conjugated IgG rabbit-specific, Alexa-fluor 488 conjugated IgG mouse-specifc, Alexa-fluor 488 conjugated IgG rat-specific and Alexa-fluor 594 conjugated IgG mouse-specific Abs (Invitrogen, goat) were used for fluorescent imaging as described[45]. Erk1/2 (rabbit), pErk1/2 (Thr202, Tyr204, mouse, clone E10, Cell Signaling)-specific antibodies and alkaline–phosphatase (AP)–labeled secondary antibodies (GE Healthcare) were used for immunoblot analyses. Rabbit anti-rat bridging antibody (Cappel #55704) was used for immunogold labeling.

Cell lines. Huh7.5.1, Huh7.5-GFP, Huh7.5 shCD81.1, 293T, HepG2 DsRed-CD81 and Caco-2 cells were cultured as described[10,46-49].

Imaging of CLDN1 in human and chimeric livers. Chimeric mouse and human liver samples were formalin fixed and paraffin embedded. Human liver tissue was obtained from patients undergoing liver transplantation due to HCV or from normal livers taken

from surplus donor tissue used for reduced size transplantation. Informed consent from each patient was obtained with regional ethics committee approval (project number 04/Q2708/40). Sections were subjected to low temperature antigen retrieval pre-treatment, followed by fluorescent detection of CLDN1, CD10 or CK18 as previously described[45]. Labeled sections were visualized using laser scanning confocal microscopy (Zeiss LSM 780, 100 x Plan Apochromat 1.4NA oil immersion objective). Background and autofluorescence of tissue samples were corrected throughout and 3D composite images were generated using the Zeiss Zen analysis software.

Transmission electron microscopy and immunogold labeling of CLDN1 *in vivo*. Human liver-chimeric mice were injected with 500 µg control or CLDN1-specific mAb and sacrificed 5h later. Mice were perfused with PBS for 3 min through portal vein infusion followed by 5 min perfusion with 4% electron microscopy (EM)-grade paraformaldehyde (PFA). Livers were harvested, minced in 3 mm pieces and fixed in 4% PFA at room temperature for 24h. Subsequently liver pieces were placed in PBS and kept at 4°C before processing for EM. Prior to freezing in liquid nitrogen the tissue were infiltrated with 2.3M sucrose in PBS containing 0.2M glycin for 15 min. Frozen samples were sectioned at -120°C, the sections were transferred to formvar-carbon coated copper grids. Grids were floated on PBS at room temperature (RT) until the immunogold labeling was carried out at RT on a piece of parafilm using CLDN1-specific mAb, rabbit anti-rat bridging antibody and 15nm Protein-A gold. Contrasting/embedding of the labeled grids was carried out on ice in 0.3% uranyl acetete in 2% methyl cellulose

for 10 min. Grids were examined in a JEOL 1200EX Transmission electron microscope and images were recorded with an AMT 2k CCD camera.

CLDN1 staining on polarized HepG2 cells. HepG2 DsRED-CD81 cells were grown on 13 mm diameter borosilicate glass coverslips at $4x10^4$ cells/coverslip (Fisher Scientific, UK). Laser scanning confocal microscopy (LSCM) was performed on a Zeiss Meta Head Confocal Microscope with a 63x water immersion objective. For live cell receptor staining of CD81 and CLDN1 in HepG2 DsRED-CD81 cells, cells were washed twice with PBS before blocking in PBS-BSA-0.01% sodium azide (Sigma, UK) for 15 min. Cells were incubated with the following primary antibodies: anti-CD81 (1µg/mL) and anti-CLDN1 (1:200) in PBS-BSA-azide for 30 min at 37°C. Cells were washed 3x in PBS before fixing with 3.6% PFA for 30 min. Cells were washed 3x with PBS before addition of a goat anti-mouse secondary Ab (Alexa 488, Invitrogen) at a 1:1000 dilution in PBS-BSA-azide or a goat anti-rat secondary Ab (Alexa 488, Invitrogen) for 30 min at 37°C. Cells were then washed with PBS before mounting and visualization.

Human liver-chimeric mice. Human liver-chimeric mice were produced by transplanting cryopreserved human hepatocytes into the spleen of 3 week-old homozygous urokinase-type plasminogen activator-transgenic Severe Combined Immuno-Deficiency-beige of both sex (uPA-SCID-bg) mice[8,15].

***In vivo* experimentation**. For prevention studies, chimeric uPA-SCID mice were intraperitoneally injected with 500 µg CLDN1-specific or control mAb at day -1 before and days 1 and 5 after inoculation of a genotype 1b or 4 HCV-infected serum. HCV infection was performed as previously described[8]. For treatment studies, chimeric uPA-SCID mice were chronically infected with HCVcc of prototype strain Jc1[22], a genotype 1b/2a chimeric VL-JFH1[27] or genotype 2a and 4 serum. Chronically infected mice received 500 µg CLDN1-specific or control mAb once a week for 4 weeks, except for genotype 4 where mice received 2 injections per week throughout the study period. Blood was harvested by retro-orbital puncture under general anesthesia. Experiments were performed in the Inserm Unit 1110 animal facility according to local laws and ethical committee approval (AL/02/19/08/12 and AL/01/18/08/12).

Viral load. Viral load was quantified using Abbott RealTime™ HCV assay (Abbott). The linear range of the assay is 12 IU/mL to 10^8 IU/mL, the limit of quantification (LOQ) of HCV RNA is 12 IU/mL. Given a mouse serum dilution of 1:100 in PBS, LOQ is 1200 UI/mL, i.e. 5160 copies/mL.

Analysis of CLDN1-specific mAb serum concentrations. Serum antibody concentrations were quantified using a rat IgG2b antibody-specific ELISA (ref. E110-111, Bethyl Laboratories, Euromedex) following the recommendations of the supplier.

Liver biopsies. Eligible patients were identified by a systematic review of patient charts at the Hepatology outpatient clinic of the University Hospital of Basel, Switzerland. The protocol was approved by the Ethics Committee of the University Hospital of Basel, Switzerland. Written informed consent was obtained from all patients. Histopathological grading and staging of the HCV liver biopsies according to the Metavir classification system was performed at the Pathology Institute of the University Hospital Basel and are summarized in Supplementary Table 3. All patients that donated liver tissue were male between 27 and 61 years old and female between 39 and 62 years old (Supplementary Table 4). Liver biopsy tissues from patients were analyzed as described[50]. In brief, liver tissue was lysed in 100 mM NaCl, 50 mM Tris pH 7.5, 1 mM EDTA, 0.1 % Triton X-100, 10 mM NaF, 1 mM PMSF, and 1 mM sodium ortho-vanadate during mechanic homogenization followed by 20 min incubation on ice. Lysates were cleared by centrifugation at 4 °C and 21,000 x g for 5 min prior to immunoblot analysis of 5 µg protein per sample. For *ex vivo* stimulation, fresh liver biopsies were divided in two equal pieces and incubated for 4h at 37°C in DMEM medium supplemented with 10 % fetal calf serum and 100 µg/mL control or CLDN1-specific mAb, respectively.

Analysis of protein expression and phosphorylation. Immunoblots of cell lysates using Erk1/2-specific antibodies were performed using Hybond–P membranes and visualized using ECF substrate (GE Healthcare) according to the manufacturer's protocol. Fluorescence emission was detected using Typhoon Trio high performance fluorescence scanner (GE Healthcare) and quantified using Image Quant TL software

(GE Healthcare). Phospho-array analysis was performed using Proteome Profiler Human Phospho-kinase Array (R&D Systems) as described by the manufacturer. For imaging, blots were incubated with ECL (GE Healthcare) and exposed to ECL Hyperfilm (GE Healthcare). Phospho-kinase array results were quantified by integrating the dot blot densities using Image J software (NIH).

Inhibition of HCV infection by protein kinase inhibitors. Huh7.5.1. cells were plated in 96 well-plates (2 x 10^3 cells/well) and infected 24h later for 3 days with HCVcc Luc-Jc1. Medium was then removed and replaced with medium containing 10 µM erlotinib (LC Laboratories) or UO126 (Calbiochem) and final concentration of 1% DMSO. Control medium contains only 1% DMSO. Three days later, HCV replication was quantified by luciferase activity measurement.

EGF-induced MAPK activation. Huh7.5.1 cells were serum starved for 4h prior 1h incubation with 100 µg/mL control or CLDN1-specific mAb and 15 min incubation with increasing concentrations (1, 10 and 100 ng/mL) of EGF. P-EGFR, p-Erk1/2 and total Erk were detected by Western blotting. Quantification was performed using a Typhoon Trio laser scanner and ImageQuant Software (GE Healthcare).

FISH analyzes of human chimeric livers. Liver samples from mice were collected during necropsy, immediately embedded in optimal cutting temperature compound (OCT) and frozen in liquid nitrogen chilled 2-methylbutane. Tissues were then stored at

-80°C until use. Sections (10 µm) were cut at cryostat (Leica), fixed overnight in 4% formaldehyde at 4°C and hybridized, as previously described[39], with the following modifications. Briefly, tissue sections were pre-treated by boiling (90°-95°C) in pre-treatment solution (Affymetrix – Panomics) for 1 min, followed by a protease QF (Affymetrix – Panomics) digestion for 10 min at 40°C. Hybridization was performed using probe sets against JFH-1 HCV RNA (target region 4513-6253) and against human GAPDH mRNA (VA6-12786-06, Affymetrix-Panomics). Pre-amplification, amplification and detection were performed according to provider's protocol. Images were acquired with a LSCM (LSM710, Carl Zeiss Microscopy, Göttingen, Germany) and Zen2 software, using same settings for all the tissues analyzed. Five to seven random fields were selected from each section, based only on the presence of human GAPDH signal to ensure the presence of human hepatocytes. Images were then acquired also including the channel for the HCV detection. Image analysis was performed using ImageJ and CellProfiler software, with a customized pipeline. Total number of cells, number of human hepatocytes (HH), number of HCV+ HH and HCV signal average intensity (and s.d) were evaluated.

Statistical analyzes. For *in vivo* and *ex vivo* data, the one-way ANOVA followed by Tukey's Post-Hoc test or the Kruskall-Wallis followed by Dunn's Post Hoc test were used after determination of distribution by the Shapiro-Wilk normality test. The Wilcoxon rank test as well as the two-tailed Mann-Whitney test were also used. The *in vitro* data are presented as the mean ± s.d. except where mean ± s.e.m. is indicated, and were

analyzed by the unpaired Student's t-test or the two-tailed Mann-Whitney test as indicated. A *p*-value ≤ 0.05 was considered significant. Statistical analyzes were performed with GraphPad Prism 6 software.

SUPPLEMENTARY METHODS REFERENCES

45. Reynolds, G.M., et al. Hepatitis C virus receptor expression in normal and diseased liver tissue. Hepatology 47, 418-427 (2008).

46. Koutsoudakis, G., Herrmann, E., Kallis, S., Bartenschlager, R. & Pietschmann, T. The level of CD81 cell surface expression is a key determinant for productive entry of hepatitis C virus into host cells. J Virol 81, 588-598 (2007).

47. Harris, H.J., et al. CD81 and claudin 1 coreceptor association: role in hepatitis C virus entry. J Virol 82, 5007-5020 (2008).

48. Piche, T., et al. Impaired intestinal barrier integrity in the colon of patients with irritable bowel syndrome: involvement of soluble mediators. Gut 58, 196-201 (2009).

49. Zahid, M.N., et al. The postbinding activity of scavenger receptor class B type I mediates initiation of hepatitis C virus infection and viral dissemination. Hepatology 57, 492-504 (2013).

50. Dill, M.T., et al. Interferon-gamma-stimulated genes, but not USP18, are expressed in livers of patients with acute hepatitis C. Gastroenterology 143, 777-786 e771-776 (2012).

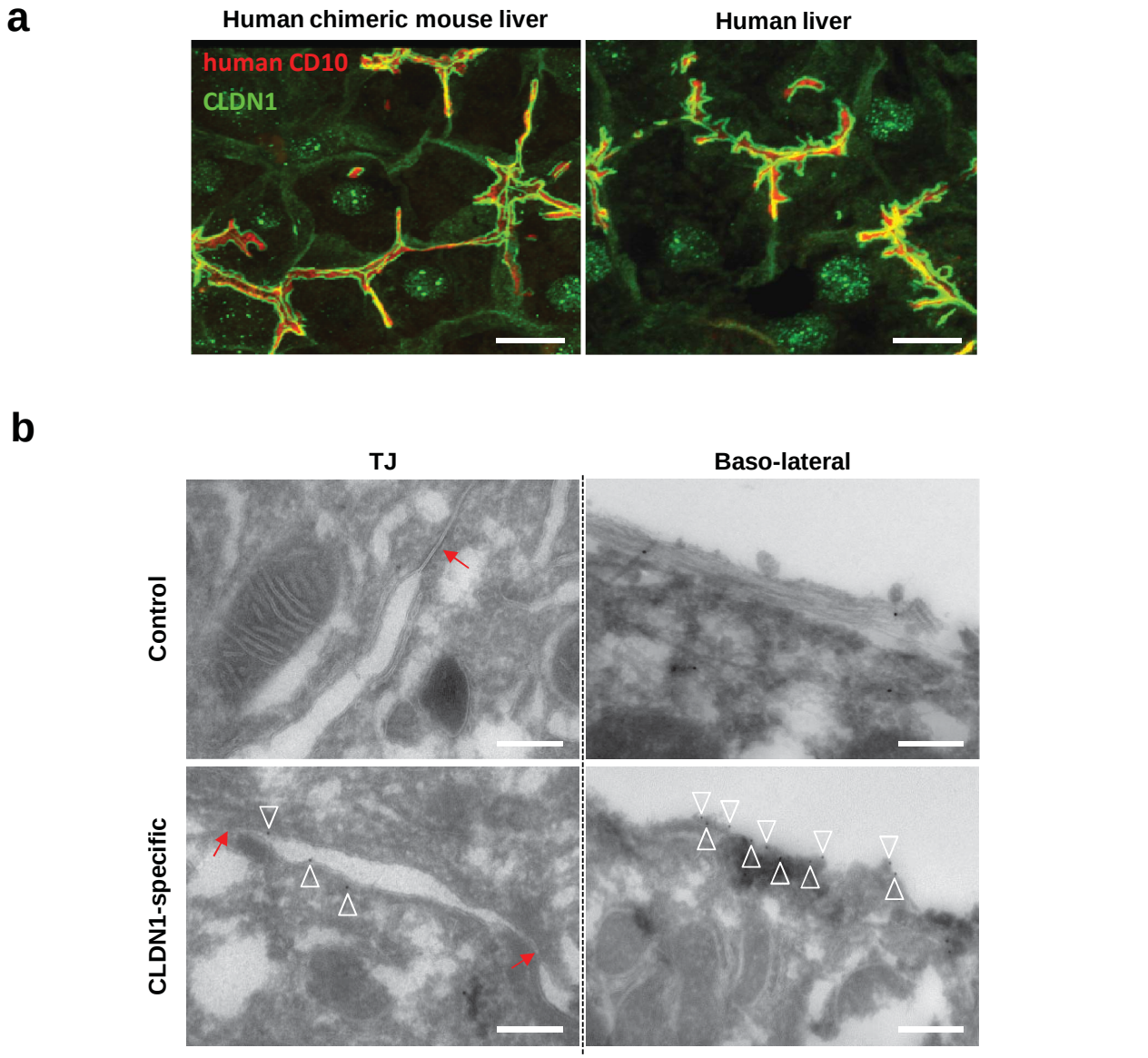
a
Human chimeric mouse liver
Human liver
human CD10
CLDN1
b
TJ
Baso-lateral
Control
CLDN1-specific
c
DsRED-CD81
Specific mAb
Merge
Anti-CD81
Anti-CLDN1

Figure 1

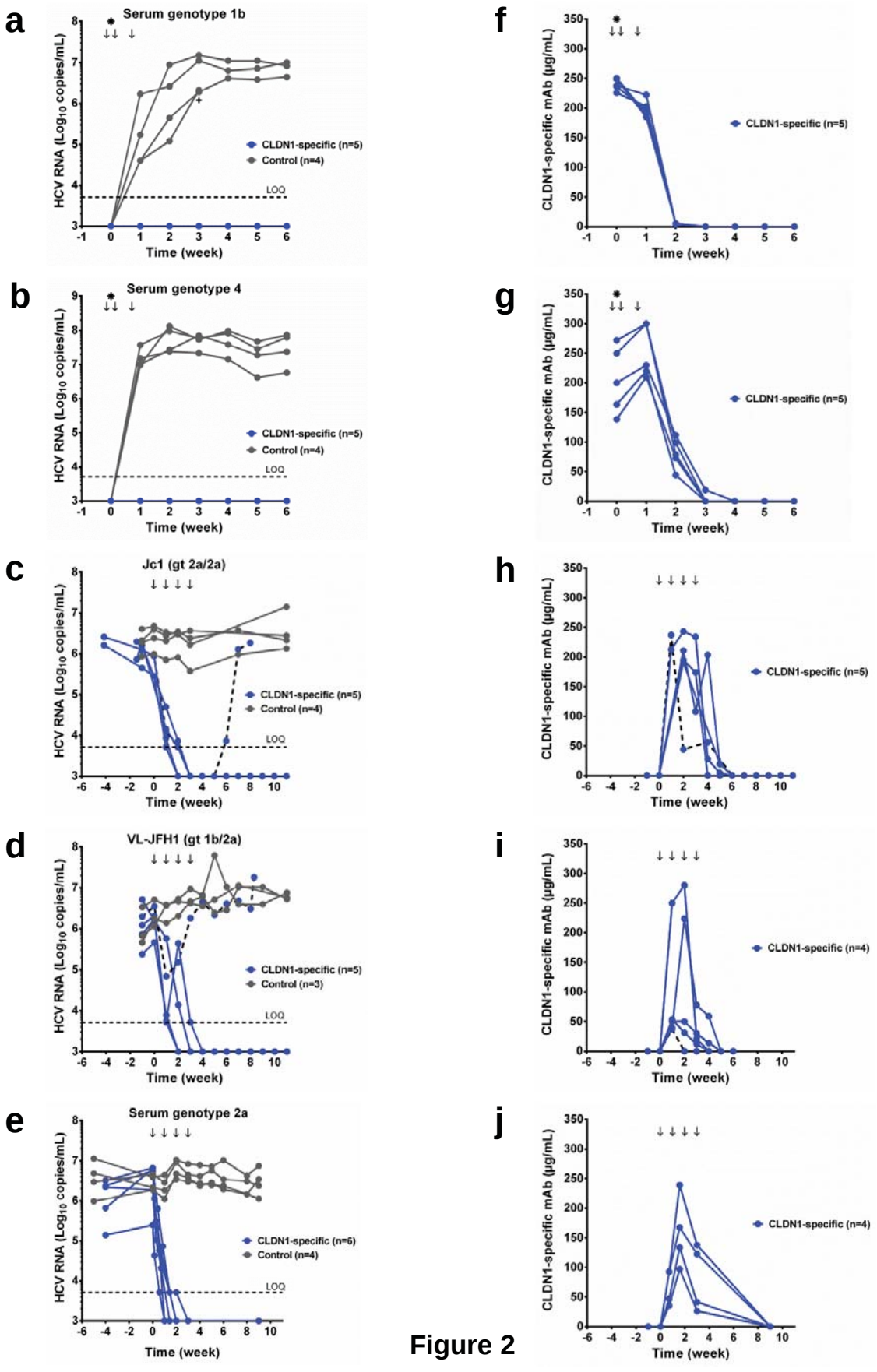
a
Serum genotype 1b
HCV RNA (Log10 copies/mL)
Time (week)
CLDN1-specific (n=5)
Control (n=4)
LOQ
f
CLDN1-specific mAb (μg/mL)
Time (week)
CLDN1-specific (n=5)
b
Serum genotype 4
HCV RNA (Log10 copies/mL)
Time (week)
CLDN1-specific (n=5)
Control (n=4)
LOQ
g
CLDN1-specific mAb (μg/mL)
Time (week)
CLDN1-specific (n=5)
c
Jc1 (gt 2a/2a)
HCV RNA (Log10 copies/mL)
Time (week)
CLDN1-specific (n=5)
Control (n=4)
LOQ
h
CLDN1-specific mAb (μg/mL)
Time (week)
CLDN1-specific (n=5)
d
VL-JFH1 (gt 1b/2a)
HCV RNA (Log10 copies/mL)
Time (week)
CLDN1-specific (n=5)
Control (n=3)
LOQ
i
CLDN1-specific mAb (μg/mL)
Time (week)
CLDN1-specific (n=4)
e
Serum genotype 2a
HCV RNA (Log10 copies/mL)
Time (week)
CLDN1-specific (n=6)
Control (n=4)
LOQ
j
CLDN1-specific mAb (μg/mL)
Time (week)
CLDN1-specific (n=4)

Figure 2

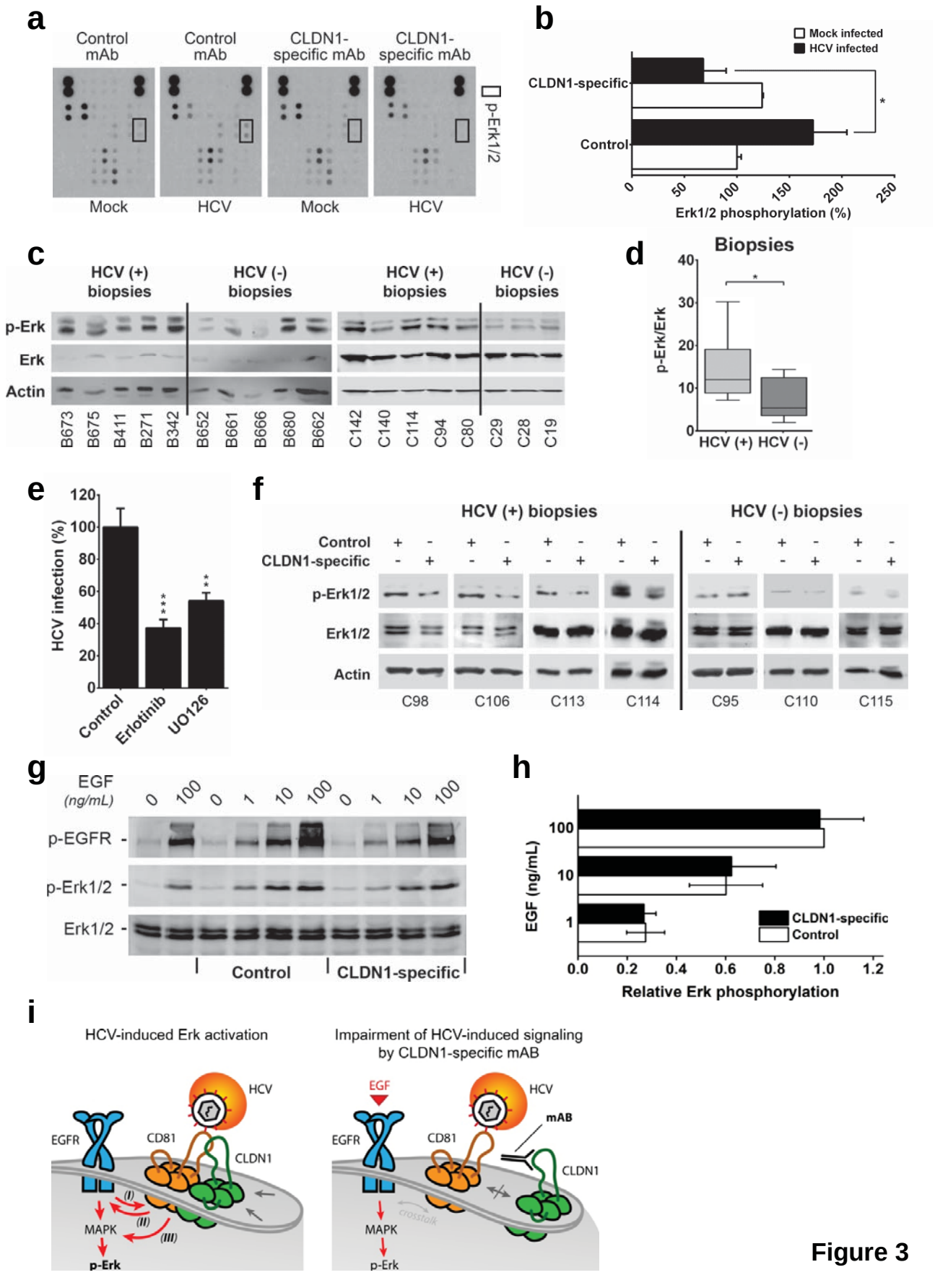
a
Control mAb
Control mAb
CLDN1-specific mAb
CLDN1-specific mAb
p-Erk1/2
Mock
HCV
Mock
HCV
b
Mock infected
HCV infected
CLDN1-specific
Control
*
0
50
100
150
200
250
Erk1/2 phosphorylation (%)
c
HCV (+) biopsies
HCV (-) biopsies
HCV (+) biopsies
HCV (-) biopsies
p-Erk
Erk
Actin
B673 B675 B411 B271 B342 B652 B661 B666 B680 B662 C142 C140 C114 C94 C80 C29 C28 C19
d
Biopsies
p-Erk/Erk
40
30
20
10
0
*
HCV (+)
HCV (-)
e
HCV infection (%)
120
100
80
60
40
20
0
***
**
Control
Erlotinib
UO126
f
HCV (+) biopsies
HCV (-) biopsies
Control
CLDN1-specific
p-Erk1/2
Erk1/2
Actin
C98 C106 C113 C114 C95 C110 C115
g
EGF (ng/mL)
0 100 0 1 10 100 0 1 10 100
p-EGFR
p-Erk1/2
Erk1/2
Control
CLDN1-specific
h
EGF (ng/mL)
100
10
1
CLDN1-specific
Control
0.0 0.2 0.4 0.6 0.8 1.0 1.2
Relative Erk phosphorylation
i
HCV-induced Erk activation
Impairment of HCV-induced signaling by CLDN1-specific mAB
HCV
EGFR
CD81
CLDN1
(I)
(II)
(III)
MAPK
p-Erk
EGF
HCV
mAB
EGFR
CD81
CLDN1
crosstalk
MAPK
p-Erk

Figure 3

a

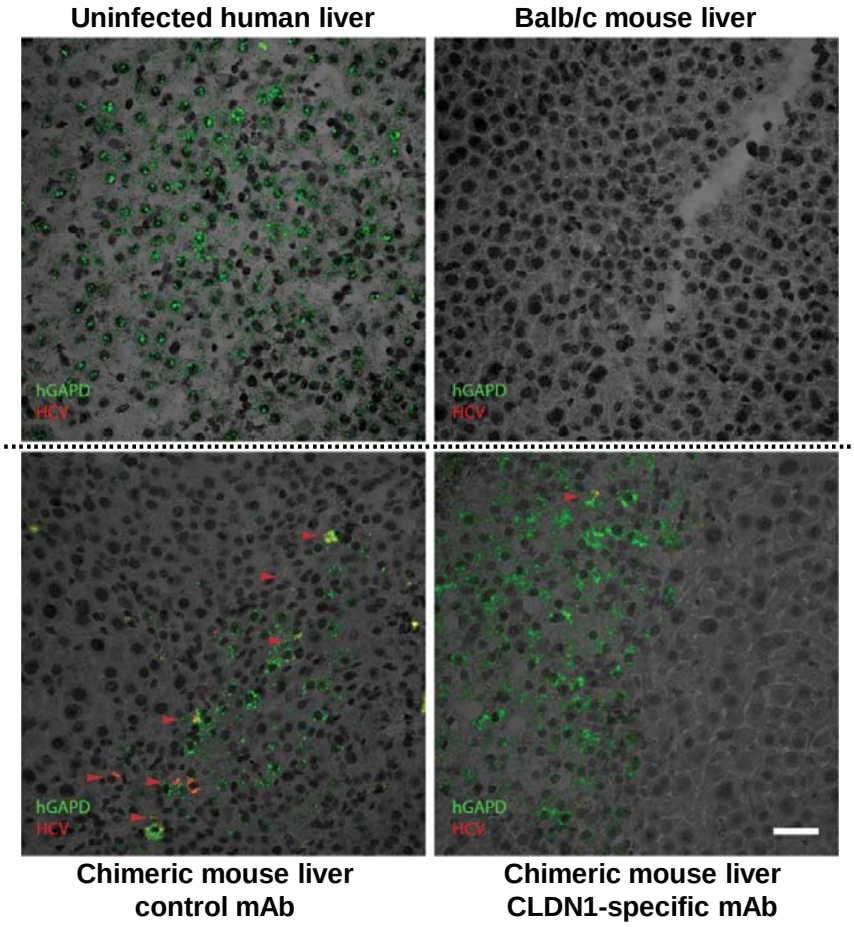
Uninfected human liver
Balb/c mouse liver
hGAPD
HCV
hGAPD
HCV
hGAPD
HCV
hGAPD
HCV
Chimeric mouse liver
control mAb
Chimeric mouse liver
CLDN1-specific mAb

b

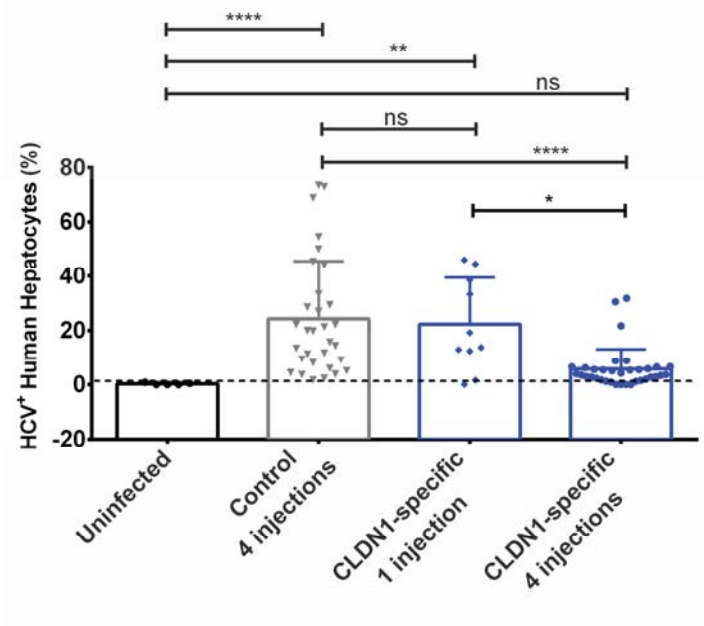
****
**
ns
ns
****
*
HCV+ Human Hepatocytes (%)
80
60
40
20
0
-20
Uninfected
Control
4 injections
CLDN1-specific
1 injection
CLDN1-specific
4 injections

Figure 4